Semiquantal treatment of excited-atom–excited-atom collisions

M. R. Flannery and K. J. McCann
School of Physics, Georgia Institute of Technology, Atlanta, Georgia 30332
(Received 18 December 1978)

The semiquantal treatment of collision processes such as $H(nl) + H(n_0l_0) \rightarrow H(n'l') + H^+ + e$ is described. The associated cross sections display systematic trends in the distribution over final angular momentum states in keeping with those previously predicted for e-H(nl) inelastic collisions. Deexcitation between close-neighboring levels n and n' of the projectile (with simultaneous ionization of the target) is generally more rapid than the endothermic processes involving the reverse transition in the projectile and, as n is increased, becomes quite competitive with those processes associated with no internal-energy change in the projectile, particularly at the lower impact energies. The cross sections, with appropriate statistical weights, for forward and reverse transitions in the projectile tend to the same high-energy limit.

I. INTRODUCTION

For variation of the quantum numbers in the single $nl \rightarrow n'l'$ transitions occurring in e-H(nl) and H($1s$)-H(nl) collisions, recent theoretical developments[1,2] have shown that the maximum cross section, with respect to impact energy E, in general oscillates on a background which continually rises, until it attains a pronounced peak at a unique value l'_{max} which is strongly dependent only on the initial principal quantum number n and which is fairly insensitive to changes in l and l'. For accessible values of $l' > l'_{max}$, the cross section exhibits a sharp marked reduction, despite increase of the $(2l'+1)$ degeneracy factor, and diminishes extremely rapidly with further increase in l'. From consideration of overlap of the corresponding momentum wave functions (which provides the inelastic form factor), the following expression for l'_{max} can be deduced[1]:

$$l'_{max} = \min\left\{(n'-1),\ \sim\left[n\left(\frac{2(n+3)}{n+1}\right)^{1/2} - \frac{1}{2}\right]\right\}, \quad (1)$$

valid in the limit $n' \gg n \gg 1$. The main feature is not so much the character (dipole, quadrupole, etc.) of the transition as is the value of l'_{max} which is primarily n dependent. Whether or not this l'_{max} includes or precludes a dipole transition is only of secondary importance. For example, transitions between the $n = 10$ and 20 levels are dominated by the $10l \rightarrow 20(l'_{max} \sim 15)$ array, none of which have dipole character. In cases where the array include some with dipole character, i.e., $l = l'_{max} \pm 1$, then these dipole transitions tend only to be somewhat more probable, although the full array $nl \rightarrow n'l'_{max}$ are the main contributors to transitions between levels n and n'.

In the semiquantal treatments previously proposed[3-5] for neutral-neutral collision processes involving excited states, as in, for example,

$$A(nl) + B(n_0l_0) \rightarrow A(n'l') + B^+ + e, \quad n_0 > n, \quad (2)$$

the scattering of the Rydberg electron of B by the incoming atom A plays a key role. Here, electron ejection from the target atom B, initially in a highly excited state with quantum numbers n_0l_0 is achieved via a collision of this valence electron with the (excited) projectile atom A originally in state with quantum numbers nl. The treatment[3] has also been generalized[4] so as to include the possibility of simultaneous transitions $nl \rightarrow n'l'$ in the projectile. Such transitions are theoretically acknowledged by use of the differential cross section for corresponding e-$A(nl)$ inelastic scattering into regions of angular and velocity space as determined by the overall required internal-energy change.

In light of the interesting predictions noted above for e-H(nl) inelastic collisions, it is of interest to determine whether or not these systematic trends are preserved in processes such as those in (2), where the electron-atom inelastic cross section, although somewhat modified, is an explicit ingredient. The present investigation is therefore an attempt (a) to explore the extent to which processes (2) reflect the basic regularities previously obtained[1,2] for $nl \rightarrow n'l'$ collisional cross sections, (b) to probe the variation with n of the deduced cross sections which should display, where appropriate, the essential endothermic or exothermic character of processes (2), and (c) to determine whether or not the cross sections for the endothermic process involving target-ionization and possible excitation of the projectile, in general exceed those for exothermic cases associated with suitable deexcitation of $A(nl)$. Moreover, collisional mixing between different angular states associated with a given principal quantum number n will also be investigated.

II. SEMIQUANTAL TREATMENT

In this treatment the differential cross section for a collision, at relative speed v, between an incoming atomic or molecular species A of mass M_A and a highly excited atom B in quantum state $|nl\rangle$ is[4]

$$\frac{d\sigma}{d\epsilon}(\epsilon,\Delta;v)=\frac{1}{v^2}\int_0^\infty u^{-1}\mathcal{F}_0(u)du \times\int_{g^-}^{g^+}\gamma^{-1}(v,u,g)g^2\,dg \times\int_{\psi^-}^{\psi^+}\frac{\omega^{-1}\sigma_{eA}(g,\psi)d(\cos\psi)}{[(\cos\psi^+-\cos\psi)(\cos\psi-\cos\psi^-)]^{1/2}}, \quad (3)$$

where the gain of between ϵ and $\epsilon+d\epsilon$ in the internal energy of B is accompanied by a change Δ (positive for excitation and negative for deexcitation) in the initial energy of the projectile A. The ionic core B^+ of mass M_B^+ is ignored in this description, except insofar as it generates a (normalized) distribution $\mathcal{F}_0(u)$ in orbital speed u of the valence electron e (of mass m) obtained from the momentum wave function appropriate to the initial state n_0l_0. The interaction between this Rydberg electron and the neutral projectile is theoretically acknowledged by the quantal differential cross section $\sigma_{eA}(g,g',\psi)$ for e-$A(nl)$ elastic or inelastic scattering through angle ψ (in the e-A center-of-mass reference frame), g and g' being relative e-A speeds before and after the encounter such that Δ, the change in internal energy of A, is $\frac{1}{2}M_{eA}(g^2-g'^2)$. In addition to these quantal ideas, details of the scattering (g,ψ) region accessible for specified changes ϵ, and Δ in the internal energies of target and projectile are provided by classical arguments, such that the overall treatment is termed semiquantal. It can be shown[6] that Eq. (3) follows also from a quantal impulse approximation, valid for highly excited state processes as formula (2).

In order to achieve the desired energy changes ϵ and Δ consistent with the three initial speeds v, u, and g, the e-A scattering is confined to within angular limits $\psi^\pm$ specified by[4]

$$\cos\psi^\pm(g,u;v)=\omega^{-1}\gamma^{-2}\{\alpha(\alpha+\xi)\pm\beta[\omega^2\gamma^2-(\alpha+\xi)^2]^{1/2}\}, \qquad \omega=g'/g, \quad (4)$$

in which the parameters

$$\alpha=\tfrac{1}{2}M_{eA}\{u^2-v^2+[(1-a)/(1+a)]g^2\}, \quad (5)$$

$$\beta=\tfrac{1}{2}M_{eA}[g^2(2u^2+2v^2-g^2)-(u^2-v^2)^2]^{1/2}, \quad (6)$$

and

$$\gamma=(\alpha^2+\beta^2)^{1/2} \quad (7)$$

reflect the physical conditions prior to the binary encounter. The energy changes ϵ and Δ may be conveniently assimilated in Eq. (4) by the parameter

$$\xi=\epsilon+[a/(1+a)]\Delta, \quad (8)$$

where the mass-ratio in Eqs. (5) and (8) is

$$a=M_AM_B^+/m(M_A+M_B^++m). \quad (9)$$

Although the above expressions are quite general for all masses of the interacting and spectator particles, advantage can be taken of the smallness of m with respect to M_A and M_B^+ such that $(1-a)/(1+a)$ in Eq. (5) is ~ -1. In order that $\psi^\pm$ in Eq. (3) be real, the limits to the relative speed g are[4]

$$g_1=\max(g^-,G^-) \quad (10)$$

and

$$g_2=\min(g^+,G^+). \quad (11)$$

Here

$$g^\pm=|u\pm v| \quad (12)$$

provide the range in relative speed before the $(e$-$A)$ collision, and

$$G^\pm=(U^2\pm V^2+2\Delta/M_{eA})^{1/2} \quad (13)$$

are the corresponding limits after the collision when the final speeds of e and A are, respectively,

$$U=\left(u^2+\frac{2\epsilon}{m(1+m/M_B^+)}\right)^{1/2} \quad (14)$$

and

$$V=[v^2-2(\epsilon+\Delta)/M_{AB}]^{1/2}, \quad (15)$$

where the reduced mass of any (i,j) pair of particles is M_{ij}.

The cross section for processes such as formula (2), in which electron ejection from B is accompanied by transitions in A, is therefore the four-dimensional integral

$$Q(\Delta;v)=\int_{\epsilon=I}^{\epsilon_{\max}}\frac{d\sigma}{d\epsilon}(\epsilon,\Delta;v)\,d\epsilon, \quad (16)$$

in general, where I is the ionization potential of B, and $\epsilon_{\max}$ is the maximum energy $(\frac{1}{2}M_{AB}v^2-\Delta)$ available for ionization. In order to determine the most efficient means of integration for a given case, the method can be suitably reformulated so as to reflect changes in the order of integration. Also, the above ordered set of (ϵ, u, g, and ψ) variables can be transformed to the alternative ordered set (ϵ, u, P, and g) which introduces the momentum change

$$P=M_{eA}(g^2+g'^2-2gg'\cos\psi)^{1/2} \quad (17)$$

explicitly rather than the scattering angle ψ. This procedure yields, after much analysis,[4]

$$\frac{d\sigma}{d\epsilon}=\frac{2}{M_{eA}^2v^2}\int_0^\infty u^{-1}\mathfrak{F}_0(u)\,du \times\int_{P^-}^{P^+}dP\int_{g_1}^{g_2}\frac{g\omega^{-1}\sigma_{eA}(P,g)\,dg}{[(g_2^2-g^2)(g^2-g_1^2)]^{1/2}}\,, \tag{18}$$

where, for specified u and ϵ, the limits to the momentum-change P are

$$P^-(u,\epsilon;v,\Delta)=\max[M|U-u|,M_{AB}|V-v|]\,,$$
$$M=m(1+m/M_B^+) \tag{19}$$

and

$$P^+(u,\epsilon;v,\Delta)=\min[M(U+u),M_{AB}(V+v)] \tag{20}$$

which ensure real limits $g_{1,2}$ (which depend on P, u, ϵ, v, and Δ and need not be given here) to g.

The chief limitation to application of this treatment is however imposed by availability of differential cross sections for e-A elastic or inelastic scattering. In the limit of high n_0l_0 and low incident speeds v, the elastic scattering can be considered as isotropic such that the inner integral in Eq. (3) is simply $\pi\omega^{-1}\sigma_{eA}(g)$. It is this feature which suggests that measurement of neutral-excited atom collisions could possibly furnish, if properly unfolded from Eq. (3), data on electron-atom collisions at extremely low energies, information prohibitively difficult to obtain via direct techniques. Also in the limit of high incident speeds v, or energy E much greater than the transition energy ΔE, the Born approximation to $(e$-$A)$ scattering can be used with considerable simplification. Since the Born scattering amplitude $f_{nl,n'l'}(P)$ is a function of momentum change P alone, expression (18) is simplified to give

$$\frac{d\sigma}{d\epsilon}(\epsilon;v,\Delta)=\frac{\pi}{M_{eA}^2v^2}\int_0^\infty u^{-1}\mathfrak{F}_0(u)\,du \times\int_{P^-}^{P^+}|f^B_{nl,n'l'}(P)|^2\,dP \tag{21}$$

for the cross section for simultaneous electron-ejection per unit energy interval about energy transfer ϵ accompanied by the transition $nl\to n'l'$ in the projectile.

We note that the integral cross section for pure electron-projectile collisions at relative speed g is

$$Q_{nl,n'l'}(g)=\frac{2\pi}{M_{eA}^2v^2}\int_{M_{eA}|g-g'|}^{M_{eA}(g+g')}|f^B_{nl,n'l'}(P)|^2P\,dP \tag{22}$$

which, by comparison with (21), suggests that the semiquantal description of A-$B(n_0l_0)$ collisions emphasizes the role of smaller momentum changes more strongly (by a factor of P^{-1}) than does the cross section (22) for $(e$-$A)$ scattering alone. This feature is the origin of any main departure of the cross sections for (2) with different $n'l'$ from the systematic regularities previously given for $nl\to n'l'$ transitions in e-H(nl) collisions. In the limit of high energies of A-B impact, the momentum change P is small and impulsive. Thus the energy transferred to the valence electron with speed limits $\pm u$ is within the interval $d\epsilon$ given by 2 Pu which, when inserted in (21), yields (22). Hence the high-energy limit to the present treatment yields the free-collision approximation, introduced by Dimitrev and Nikolaev[7] (cf. Flannery[8]) and based on the idea that the electrons of a target appear free to a very fast incident particle, from which they acquire sufficient energy through the momentum transfer to exceed both their binding energy and possible energy of excitation of the target.

A useful analytic procedure, which shows this equivalence more rigorously, considers the limits to the energy-change ϵ resulting from fixed u and P. We therefore find after lengthy analysis that the cross section per unit momentum change, rather than unit energy change as in (18), is[4,5]

$$\frac{d\sigma}{dP}=\frac{2}{M_{eA}^2v^2}\int_0^\infty u^{-1}\mathfrak{F}_0(u)\,du \times[\epsilon^+(P,u;v,\Delta)-\epsilon^-(P,u;v,\Delta)] \times\int_{g^-}^{g^+}\frac{g\omega^{-1}\sigma_{eA}(P,g)\,dg}{[(g_2^2-g^2)(g^2-g_1^2)]^{1/2}}\,. \tag{23}$$

The energy-change limits in (23) for specified P and u are

$$\epsilon^+=\min(E_e^+,E_i^+),\quad \epsilon^-=\max(E_e^-,E_i^-)\,, \tag{24}$$

where

$$E_e^\pm=\tfrac{1}{2}(P^2/M)\pm Pu \tag{25}$$

are the kinetic energies gained by an electron of mass M and speed u as a result of an impulse $\pm P$ applied along the direction of motion, and where

$$E_i^\pm=-[\tfrac{1}{2}(P^2/M_{AB})\mp Pv+\Delta] \tag{26}$$

are the corresponding kinetic energies lost by a particle of mass M_{AB} and speed v which absorbs energy Δ as internal energy and which undergoes momentum change $\pm P$ along direction of motion. In the limit of high incident speeds v, $\epsilon^\pm$ tends to $\pm Pu$, respectively, and, on assuming $\sigma_{eA}(P,g)$ is a function only of P, Eq. (23) reduces to (dQ/dP) of Eq. (22).

The final ingredient required for application of the treatment is the quantal velocity distribution obtained from the momentum wave functions[9] for state $|nl\rangle$. For atomic hydrogen with energy ϵ_n, this can be written

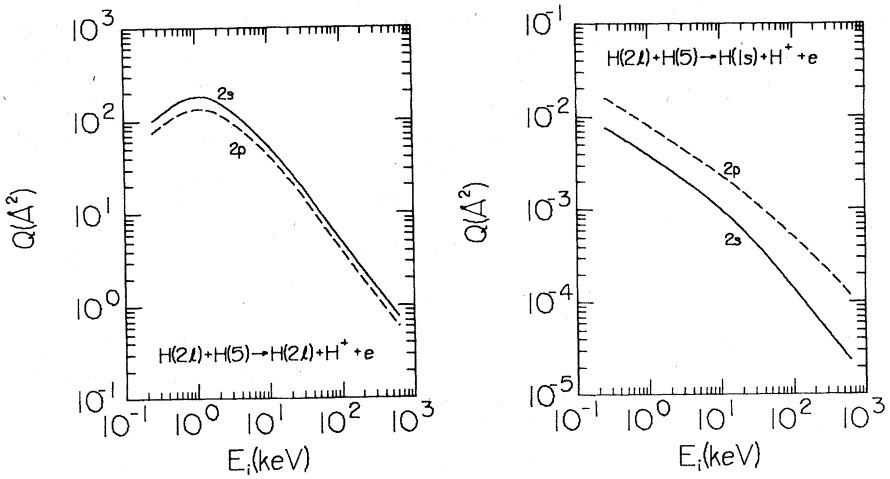

FIG. 1. Cross sections (Å^2) for H($2l$) +H($n=5$) →H($2l$, $1s$) +H$^+$ +e as a function of relative kinetic energy E_i (keV).

$$\mathcal{F}_{nl}(u)=\frac{2^{4l}(l!)^2(n-l-1)!}{(n+l)!}\frac{\lambda_n^{2l}}{(\lambda_n^2+1)^{2l}}\times[C_{n-(l+1)}^{l-1}(x_n)]^2\bar{\mathcal{F}}_n(u), \tag{27}$$

in which C_r^s are Gegenbauer polynomials with argument

$$x_n=(\lambda_n^2-1)/(\lambda_n^2+1), \tag{28}$$

where

$$\lambda_n^2=\tfrac{1}{2}Mu^2/|\epsilon_n| . \tag{29}$$

The factor

$$\mathcal{F}_{nl}(u)=\frac{32}{\pi}\left|\frac{2\epsilon_n}{M}\right|^{5/2}\frac{u^2}{(u^2+2|\epsilon_n|/M)^4}\equiv\frac{1}{n^2}\sum_{l=0}^{\infty}(2l+1)\mathcal{F}_{nl}(u) \tag{30}$$

is simply the momentum distribution averaged over the degenerate angular states l for a given hydrogenic level n. Calculation shows, for highly excited states n_0l_0 of the target, that the cross sections for processes (2) are largely independent of l_0. Therefore the function $\bar{\mathcal{F}}_n(u)$ is used throughout the subsequent investigation.

III. RESULTS AND DISCUSSION

Displayed in Fig. 1 as a function of incident relative kinetic energy E_i are the present semiquantal cross sections determined from Eqs. (3)–(30) for the collision process

$$H(2l)+H(\bar{5})\rightarrow H(2l)+H^+ +e, \quad l=0,1 , \tag{31}$$

which involves single ionization alone, the projectile left unaffected by an e-H($2l$) *elastic* encounter. Since the expectation values of r^N are larger[9] for the $2s$ state than for the $2p$ state, projectile $H(2s)$ tends to ionize somewhat more efficiently. The difference however is expected to diminish for higher n since the probability of finding an electron at a large distance from the nucleus is $\sim r^{2n+2}e^{-2r/n}$ independent of l. This information is

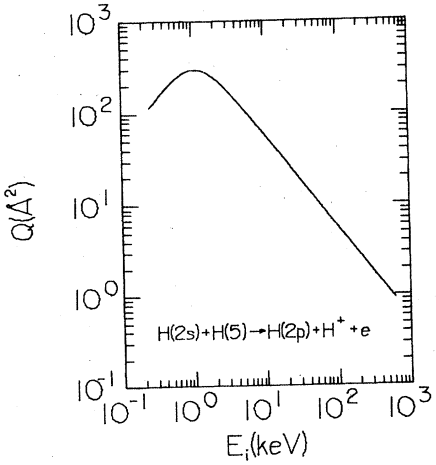

FIG. 2. Cross sections (Å^2) for H($2s$) +H($n=5$) →H($2p$) +H$^+$ +e as a function of relative kinetic energy E_i (keV).

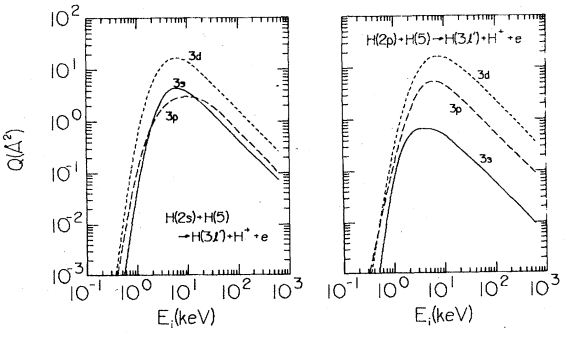

FIG. 3. Cross sections (Å^2) for H($2l$) +H($n=5$) →H($3l'$) +H$^+$ +e as a function of relative kinetic energy E_i (keV).

already contained in the Born approximation to e-H($2l$) elastic scattering. Whether it is preserved when more accurate descriptions of elastic scattering are adopted is undetermined, although the neglected effect of polarization of the projectile by the valence electron is significant only for forward-angle scattering, a region prohibited to some extent in the semiquantal cross section (3) by the presence of ψ^- in (3), the lower limit to the angular scattering. If anything, the cross section for projectile H($2s$) in Eq. (31) is expected to be further enhanced by the residual polarization effect (beyond ψ^-) thereby augmenting at low impact energies the difference between H($2s$) and H($2p$) projectiles.

Also presented in Fig. 1 are the present results for the processes

$$\mathrm{H}(2l)+\mathrm{H}(\bar{5})\rightarrow\mathrm{H}(1s)+\mathrm{H}^+ +e,\quad l=0,1\,, \tag{32}$$

which are exothermic in character owing to simultaneous deexcitation of the projectile described in this treatment by an e-H($2l$) inelastic encounter. In spite of this additional conversion of internal electronic energy, the above exothermic process is, over a wide E_i range, at least four orders of magnitude less probable than Eq. (31) for pure ionization alone. This result apparently arises from the inclusion of the $2l\rightarrow 1s$ coupling between relatively distant levels such that any advantage of the exothermic effect at lower E_i tends to be greatly offset by the weaker coupling.

When strong dipole coupling between angular momentum sublevels l is directly introduced, as in the collisional l-state mixing process,

$$\mathrm{H}(2s)+\mathrm{H}(\bar{5})\rightarrow\mathrm{H}(2p)+\mathrm{H}^+ +e \tag{33}$$

the resulting cross sections in Fig. 2 are then somewhat larger than those for pure ionization (31), particularly at lower impact-energies E_i.

As previously noted by Flannery and McCann,[1,10] the population of the $n=3$ level in e-H($2l$) collisions, and in e-He($2^{1,3}S$) collisions, is controlled, up to impact energies $\lesssim$500–1000 eV, by the transitions $2l\rightarrow 3d$, $2l\rightarrow 3s$, and $2l\rightarrow 3p$ in descending order of importance, irrespective of the initial value of l. Although weighted by an additional P^{-1} momentum-change factor, these differential cross sections for e-H($2l$) inelastic collisions are ingredients in the present semiquantal treatment of

$$\mathrm{H}(2l)+\mathrm{H}(\bar{5})\rightarrow\mathrm{H}(3l')+\mathrm{H}^+ +e\,. \tag{34}$$

Figure 3 illustrates that the above trend is indeed reflected in the cross sections for Eq. (28), i.e., the $2l\rightarrow 3d$ array dominates irrespective of l. The P^{-1} factor, however, tends to enhance those transitions which involve no angular-momentum change $\Delta l=l'-l=0$, as shown in Fig. 3. Because Eq. (34) involves transitions between relatively close levels, $n=2$ and 3, the cross sections for the endothermic process [Eq. (34)] are larger than those for the exothermic collision [Eq. (32)], but still remain smaller than those for Eqs. (31) and (33) which involve no change in internal energy of the projectile H($2l$).

Figure 4 shows that the cross sections for pure ionization

$$\mathrm{H}(3l')+\mathrm{H}(\bar{5})\rightarrow\mathrm{H}(3l')+\mathrm{H}^+ +e \tag{35}$$

are again larger (by up to six orders of magnitude) than those for the exothermic process

$$\mathrm{H}(3l')+\mathrm{H}(\bar{5})\rightarrow\mathrm{H}(nl)+\mathrm{H}^+ +e,\quad nl\equiv 2s,2p,1s\,. \tag{36}$$

Also weak couplings between distant levels, as $3l'$-$1s$, imply cross sections four orders of magnitude smaller than those for the closer $3l'$-$2l$ couplings. While the processes (36) with $n=2$ and (34) are of course not pure inverses of one another, some comparison is possible since both processes adopt electron-impact differential cross sections for $2l\rightleftharpoons 3l'$ transitions which, from (22), satisfy the detailed balance relation

$$(2l+1)E_i\,Q^{(e)}_{nl,n'l'}(E_i)$$

$$=(2l'+1)E_f\,Q^{(e)}_{n'l',nl}(E_f),\quad E_f=E_i+(\epsilon_i-\epsilon_f),$$

in which the e-atom cross sections $Q^{(e)}_{nl,n'l'}$ are averaged over the initial $(2l+1)$ degenerate states

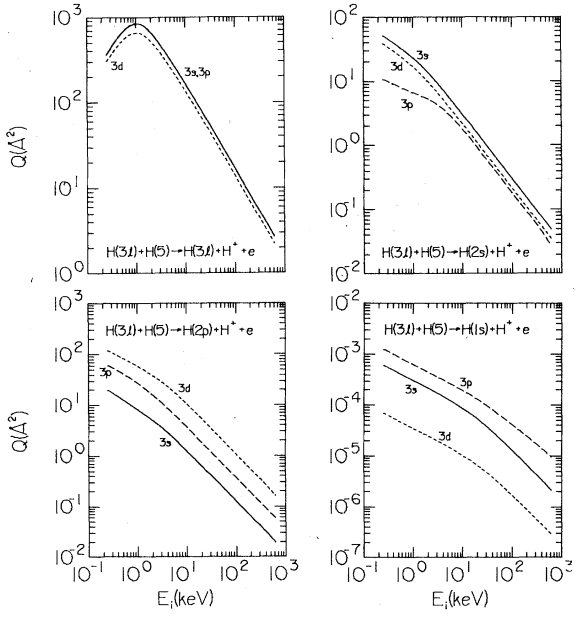

FIG. 4. Cross sections (Å^2) for H($3l$)+H($n=5$) $\rightarrow$H($3l$, $2l'$, $1s$)+H$^+$+e as a function of relative kinetic energy E_i (keV).

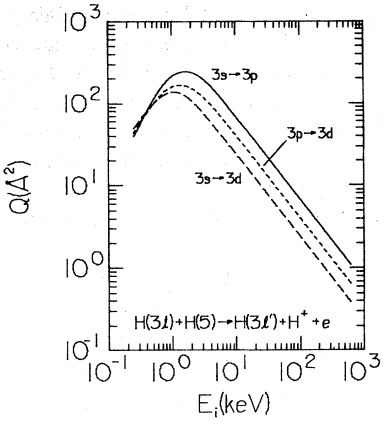

FIG. 5. Cross sections (Å^2) for H($3l$) + H($n=5$) → H($3l'$) + $H^+ + e$ as a function of relative kinetic energy E_i (keV).

of the nl level and summed over the $(2l'+1)$ final states. By multiplying the cross sections for (36) in Fig. 4 by the factor $(2l'+1)/(2l+1)$, where $l'=0$, 1, and 2, we note that the order in Fig. 3 is preserved at the higher impact energies. Moreover, as suggested by discussion following Eq. (23), these cross sections so multiplied approach the same high-energy limits as those in (34) for the forward transition in the projectile.

The cross sections in Fig. 5 for collisional angular-momentum mixing of the projectile and simultaneous ionization of the target are within an order of magnitude lower than those in Fig. 4 for pure ionization alone, and higher than the $3l \to 2l'$ exothermic cases. The dipole transitions in Fig. 5 are of course dominant since no internal energy change in the projectile is involved.

The overall trend becomes further clarified in Fig. 6 which displays cross sections for

$$\mathrm{H}(3l) + \mathrm{H}(\bar{5}) \to \mathrm{H}(4l') + \mathrm{H}^+ + e\ , \tag{37}$$

with variation of l, l' and impact-energy E_i. As illustrated by Flannery and McCann,[1] electron-impact excitation between $n=3$ and 4 levels is dominated by the $3l \to 4f$ transition array, largely independent of l. This feature, not primarily due to the increased statistical weight of the final $4l'$ state,[1] is preserved in Fig. 6 for processes (37) with one notable difference. The processes which involve no angular-momentum change with $l=l'$ in (37) gain in relative importance due to P^{-1} factor in (21) when compared with (22). While the cross sections for the endothermic $(3l \to 4l')$ processes (37) in Fig. 6 are much smaller at lower E_i than those in Fig. 4 for the exothermic $(3l \to 2l')$ processes, they are larger at very high E_i. Further, Fig. 7 shows that deactivation of the projectile to a close neighboring level accompanied by target ionization as in

$$\mathrm{H}(4l) + \mathrm{H}(\bar{5}) \to (3l') + \mathrm{H}^+ + e \tag{38}$$

become, particularly for the higher l, quite competitive with

$$\mathrm{H}(4l) + \mathrm{H}(\bar{5}) \to \mathrm{H}(4l) + \mathrm{H}^+ + e \tag{39}$$

for pure ionization alone. Also, multiplication of the cross sections in Fig. 7 for projectile deactivation by $(2l+1)/(2l'+1)$, where l' is associated with the $n=4$ level not only preserves the trend predicted in Fig. 6 for forward projectile excitation, but also yields the same high-energy limits as suggested by Eqs. (23)–(26). It is worth noting in Fig. 7 that variation of l in (39) causes little difference, as expected since for high principal quantum numbers n, the expectation values $\langle r^\nu \rangle$ for $\nu > 0$ are determined essentially by n, i.e., the probability of finding the orbital electron of the projectile at a large distance from its nucleus is essentially the some for both circular $(l=n-1)$ and the eccentric elliptical (small l) Bohr orbits.

Finally, Fig. 8 illustrates that further deactivation of the H($4l$) projectile to the $n=2$ and 1 levels yields cross sections much smaller than those in Fig. 7 for (38) and (39), in spite of the increase in exothermicity.

IV. SUMMARY AND CONCLUSION

We therefore find that the cross sections for the collision processes

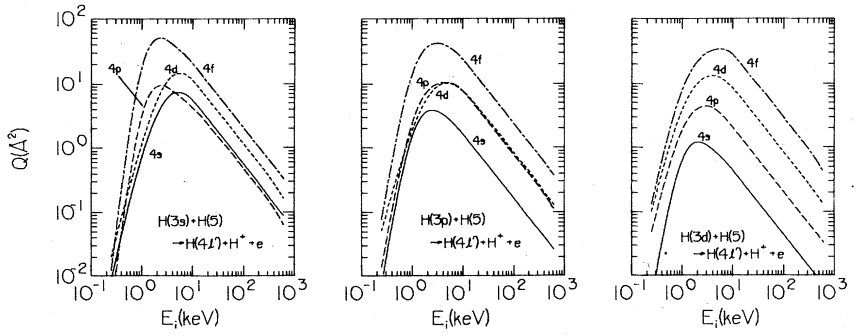

FIG. 6. Cross sections (Å^2) for H($3l$) + H($n=5$) → H($4l'$) + $H^+ + e$ as a function of relative kinetic energy E_i (keV).

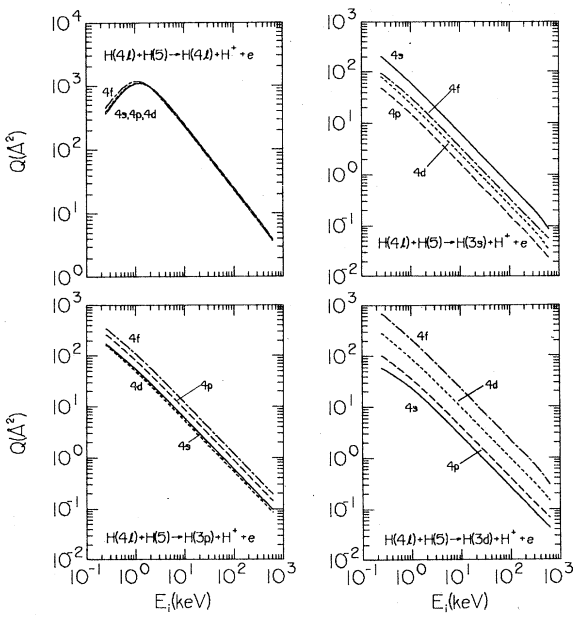

FIG. 7. Cross sections (Å^2) for H($4l$) + H($n=5$) → H($4l$, $3l'$) + H$^+$ + e as a function of relative kinetic energy E_i (keV).

$$A(nl) + B(n_0 l_0) \rightarrow A(n'l') + B^+ + e, \quad n_0 > n \qquad (40)$$

display systematic trends in the distribution over final angular momentum states l' of the projectile, in keeping with those predicted earlier[1] for e-$A(nl)$ collisions. For example, the $2l \rightarrow 3d$ and $3l \rightarrow 4f$ transition array, respectively, dominate the population of the $n'=3$ and 4 final levels of the projectile, irrespective of the initial angular momentum l. These examples indicate the emergence of the more general basic systematic pattern previously discussed[1] for the population of final angular-momentum states in e-$A(n'l')$ collisions. However, the role of small momentum change P is somewhat augmented (by the presence of the P^{-1} factor) in the semiquantal treatment for formula (40), so that transitions $nl \rightarrow n'l'$ involving no change in angular momentum of the projectile are somewhat enhanced.

The question whether exothermic processes with $n' < n$ in formula (40) are in general more probable than endothermic processes with $n' > n$ is largely determined by the energy separation between levels n and n' of the projectile. For example, in spite of the larger amount of internal energy released by the projectile in a $2l \rightarrow 1s$ transition, the associated cross sections are much smaller than those involving a $2l \rightarrow 3l'$ transition in the projectile for all impact energies E_i (except of course in the vicinity of the excitation threshold). However, the cross sections for formula (40) with $3l \rightarrow 2l'$ superelastic transitions in A are much larger than those involving the $3l \rightarrow 4l'$ excitation for all impact energies, except the highest. These cross sections remain lower than those which involve either no change or else only angular-momentum mixing by $3l \rightarrow 3l'$ transitions in the projectile. As n is increased, reverse transitions between close levels of the projectile in formula (40) are therefore not only greater than those for the forward transitions, but also become competitive with the cross sections associated with no internal-energy change in the projectile, particularly at the lower impact energies E_i. At high E_i, the cross sections with appropriate statistical weighting for forward and reverse transitions in the projectile accompanied by ionization of the target tend to same high-energy limit.

In general, the cross sections are rather large and the effects of angular-momentum redistribution among final states are sufficiently strong so as to be comparable of measurement by current experimental techniques.[11-14]

ACKNOWLEDGMENT

This research was sponsored by U. S. Department of Energy, Division of Laser Fusion, Contract No. EY-76-S-05-5002.

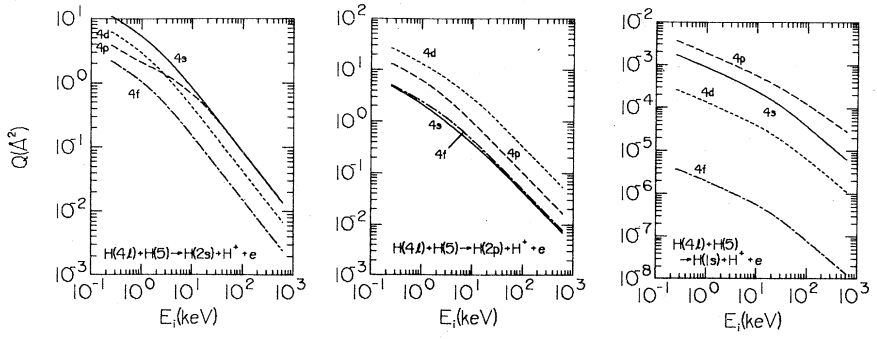

FIG. 8. Cross sections (Å^2) for H($4l$) + H($n=5$) → H($2l'$, $1s$) + H$^+$ + e as a function of relative kinetic energy E_i (keV).

[1]M. R. Flannery and K. J. McCann, J. Phys. B 12, 427 (1979).
[2]M. R. Flannery and K. J. McCann (unpublished).
[3]M. R. Flannery, Ann. Phys. (N. Y.) 61, 465 (1970).
[4]M. R. Flannery, Ann. Phys. (N. Y.) 79, 480 (1973).
[5]M. R. Flannery, J. Phys. B 8, 2470 (1975).
[6]M. R. Flannery (unpublished).
[7]I. S. Dmitriev and V. S. Nikolaev, Sov. Phys.-JETP 17, 447 (1963).
[8]M. R. Flannery, J. Phys. B 4, 892 (1971).
[9]H. A. Bethe and E. E. Salpeter, *Quantum Mechanics of One- and Two-Electron Atoms* (Springer-Verlag, Berlin, 1957), pp. 18 and 39.
[10]M. R. Flannery and K. J. McCann, Phys. Rev. A 12, 846 (1975).
[11]K. A. Smith, F. G. Kellert, R. D. Rundel, F. B. Dunning, and R. F. Stebbings, Phys. Rev. Lett. 40, 1362 (1978).
[12]T. F. Gallagher, S. A. Edelstein, and R. M. Hill, Phys. Rev. A 15, 1945 (1977).
[13]J. A. Schiavone, D. E. Donohue, D. R. Herrick, and R. S. Freund, Phys. Rev. A 16, 48 (1977).
[14]B. Anderson and E. Veje, Phys. Rev. A 16, 1980 (1977).